Available online at www.sciencedirect.com
SCIENCE DIRECT®
Journal of Magnetic Resonance 172 (2005) 133–141
JMR Journal of Magnetic Resonance
www.elsevier.com/locate/jmr

Temperature dependence of nuclear magnetization and relaxation

David H. Gultekin[a,*], John C. Gore[b]

[a] Yale University, New Haven, CT 06510, United States
[b] Vanderbilt University Institute of Imaging Science, Nashville, TN 37232, United States

Received 8 April 2004; revised 30 August 2004

Abstract

The temperature dependences of nuclear magnetization and relaxation rates are reviewed theoretically and experimentally in order to quantify the effects of temperature on NMR signals acquired by common imaging techniques. Using common sequences, the temperature dependences of the equilibrium nuclear magnetization and relaxation times must each be considered to fully understand the effects of temperature on NMR images. The temperature dependence of the equilibrium nuclear magnetization is negative because of Boltzmann's distribution for all substances at all temperatures, but the combined temperature dependences of the equilibrium magnetization and relaxation can be negative, weak or positive depending on the temperature (T), echo time (T_E), repetition time (T_R), and the temperature dependences of the relaxation times $T_1(T)$ and $T_2(T)$ in a pulse sequence. As a result, the magnitude of the NMR signal from a given substance can decrease, increase or stay somewhat constant with increasing temperature. Nuclear thermal coefficients are defined and predictions for spin echo and other simple sequences are verified experimentally using a number of substances representing various thermal and NMR properties.

Keywords: Nuclear magnetization; Relaxation; Temperature; NMR thermometry

1. Introduction

Currently, NMR imaging and spectroscopy are being developed and applied for monitoring the treatment of cancer by various physical therapies. Understanding the effects of temperature on NMR signals is important especially for the accurate application of NMR methods for monitoring thermal treatments in oncology using NMR imaging and spectroscopy. NMR imaging methods have been used to measure temperature changes within tissues but with varying degrees of success. Using conventional sequences, the temperature dependences of the nuclear magnetization and relaxation times must each be considered to quantify the effects of temperature on the NMR signals. In thermal imaging, to interpret the variations measured in NMR signals, it may be necessary to analyze the effects of temperature on each of several parameters for a given pulse sequence.

NMR signals are proportional to the nuclear magnetization and may also depend on relaxation rates, so we have evaluated the combined effects of the temperature dependences of these on the magnitude of the NMR signals acquired using common pulse sequences. We predict that although the temperature dependence of the equilibrium nuclear magnetization is negative because of Boltzmann's distribution for all substances at all temperatures, the combined temperature dependences of the equilibrium magnetization and relaxation terms for a pulse sequence can be negative, weak or positive depending on the temperature (T), echo time (T_E), repetition time (T_R), and the temperature dependences of the relaxation times $T_1(T)$ and $T_2(T)$. As a result, the magnitude of the NMR signal from a given substance

* Corresponding author. Present address: California Institute of Technology, Broad Center M/C 114-96, Pasadena, CA 91125, United States.
E-mail address: david.gultekin@aya.yale.edu (D.H. Gultekin).

1090-7807/$ - see front matter © 2004 Elsevier Inc. All rights reserved.
doi:10.1016/j.jmr.2004.09.007

can decrease, increase or stay somewhat constant with increasing temperature. The temperature dependences of the equilibrium magnetization and relaxation times may be drastically different for different substances.

While physiologic effects such as perfusion and flow are very important in thermotherapy, they are beyond the scope of this discussion. The intent of this work is to provide a theoretical and experimental analysis of the manner in which NMR signals vary with temperature in common pulse sequences.

Theoretical relations have been developed as summarized below, and the results are verified experimentally using both NMR imaging and spectroscopy. We apply these analyses to predict the temperature dependences of the NMR signal in a multi-echo (Carr-Purcell-Meiboom-Gill or CPMG) spin-echo pulse sequence, a free induction decay (FID), a spin-echo (SE) imaging and gradient-echo (GRE) imaging signal for a number of substances.

2. Theory

Temperature may affect the frequency of nuclear precession, the equilibrium magnetization, as well as rates of relaxation, and diffusion. The effect of temperature on the frequency of precession arises through thermally induced changes in the nuclear shielding [1] and its contribution to the magnitude of an NMR signal is small. The effect of spin diffusion on the magnitude of NMR signal may become apparent in the presence of large diffusion encoding field gradients. In practice, however, the effect of temperature on the magnitude of NMR signals on common sequences largely derives from the effects on the equilibrium magnetization and relaxation.

The equilibrium of nuclei with spin $= 1/2$ in a thermal reservoir and a magnetic field is governed by Boltzmann's distribution [2] which predicts that the equilibrium nuclear magnetization is

$$M(0,T) = \frac{N\gamma^2\hbar^2 I(I+1)B_0}{3k_B T}, \tag{1}$$

where N is the number of spins per unit volume, γ is the gyromagnetic ratio, $\hbar$ is Planck's constant, I is the spin quantum number, B_0 is the static magnetic field, k_B is Boltzmann's constant and T is the absolute temperature. In terms of nuclear magnetic moment, $\mu^2 = \gamma^2\hbar^2 I(I+1)$, Eq. (1) becomes

$$M(0,T) = \frac{N\mu^2 B_0}{3k_B T}, \tag{2}$$

which can be written in Curie's relation [3] as

$$M(0,T) = \chi(0,T)B_0, \tag{3}$$

where $\chi(0,T) = N\mu^2/3k_B T$ is the static nuclear paramagnetic susceptibility. Then, from Eqs. (2) and (3), we have

$$\frac{\partial M(0,T)}{\partial T} = -\frac{M(0,T)}{T} \tag{4}$$

or

$$\frac{\partial \ln M(0,T)}{\partial T} = -\frac{1}{T}, \tag{5}$$

which shows that the temperature dependence of the equilibrium nuclear magnetization is negative for all substances at all temperatures.

For a spin-echo pulse sequence [4,5]

$$M(T_E,T_R,T) = M(0,T)\,e^{-T_E/T_2(T)}\left(1 - e^{-T_R/T_1(T)}\right). \tag{6}$$

In the general case of both T_1 and T_2 weighting

$$\frac{\partial \ln M(T_E,T_R,T)}{\partial T} = -\frac{1}{T} + \frac{T_E}{T_2^2(T)}\frac{\partial T_2(T)}{\partial T} - \left(\frac{T_R}{T_1^2(T)}\frac{\partial T_1(T)}{\partial T}\right)\left(1 - e^{-T_R/T_1(T)}\right)^{-1} e^{-T_R/T_1(T)} \tag{7}$$

which shows that the temperature dependence of the signal is a function of temperature, echo time, recovery time, relaxation times, and the temperature dependences of the relaxation times $T_1(T)$ and $T_2(T)$. It is important to note that while T_E and T_R are sequence parameters not depending on the temperature, they are multipliers to the temperature dependent relaxation terms. The magnitudes of these parameters and the temperature dependences of relaxation times will therefore affect the relative sizes of the negative and positive terms in Eq. (7). In the case of so called T_2 weighting

$$T_R \gg T_1(T) \tag{8}$$

then, Eq. (7) reduces to

$$\frac{\partial \ln M(T_E,T)}{\partial T} = -\frac{1}{T} + \frac{T_E}{T_2^2(T)}\frac{\partial T_2(T)}{\partial T}. \tag{9}$$

For a gradient-echo pulse sequence with flip angle θ [4,5]

$$M(T_E,T_R,T) = M(0,T)\sin\theta\, e^{-T_E/T_2^*(T)}\left(1 - e^{-T_R/T_1(T)}\right) \times \left(1 - e^{-T_R/T_1(T)}\cos\theta\right)^{-1}. \tag{10}$$

In the case of both T_1 and T_2 weighting

$$\frac{\partial \ln M(T_E,T_R,T)}{\partial T} = -\frac{1}{T} + \frac{T_E}{T_2^{*2}(T)}\frac{\partial T_2^*(T)}{\partial T} + \cot\theta\frac{\partial\theta}{\partial T} - \frac{T_R}{T_1^2(T)}\frac{\partial T_1(T)}{\partial T}\frac{E_1}{1-E_1} - \left[\sin\theta\frac{\partial\theta}{\partial T} - \cos\theta\frac{T_R}{T_1^2(T)}\frac{\partial T_1(T)}{\partial T}\right] \times \frac{E_1}{1 - E_1\cos\theta}, \tag{11}$$

where $E_1 = e^{-\frac{T_R}{T_1(T)}}$ and $T_2^*(T)$ is the transverse relaxation time in the presence of magnetic field inhomogeneity.

The temperature dependence of the flip angle can be derived from the effects of temperature on Larmor's relation. The flip angle can be written approximately as

$$\theta = \gamma(1 - \sigma(T))B_1 t_p, \tag{12}$$

where $\sigma(T)$ is the nuclear shielding, B_1 is the transverse field and t_p is the pulse duration of the B_1 field.

Then,

$$\frac{\partial\theta}{\partial T} = -\frac{\partial\sigma(T)}{\partial T}\gamma B_1 t_p = -\frac{\partial\sigma(T)}{\partial T}\theta_0, \tag{13}$$

where $\theta_0 = \gamma B_1 t_p$ is the flip angle at some reference resonance. The temperature dependence of nuclear shielding, $\partial\sigma(T)/\partial T$, is usually very small, so the magnitude of the temperature dependence of flip angle is also very small, $|\partial\theta/\partial T| \ll 1$, and the multiplying terms can be neglected in Eq. (11).

For a flip angle of $\theta = \pi/2$, Eq. (11) then becomes

$$\frac{\partial \ln M(T_E, T_R, T)}{\partial T} = -\frac{1}{T} + \frac{T_E}{T_2^{*2}(T)}\frac{\partial T_2^*(T)}{\partial T} - \frac{T_R}{T_1^2(T)}\frac{\partial T_1(T)}{\partial T}\frac{E_1}{1 - E_1} \tag{14}$$

for the GRE pulse sequence, which is the same as Eq. (7), the temperature dependence of NMR signal in a SE pulse sequence, with only $T_2(T)$ replaced with $T_2^*(T)$ in Eq. (14).

In the absence of T_1 weighting

$$T_R \gg T_1 T \tag{15}$$

and Eq. (14) simplifies to

$$\frac{\partial \ln M(T_E, T)}{\partial T} = -\frac{1}{T} + \frac{T_E}{T_2^{*2}(T)}\frac{\partial T_2^*(T)}{\partial T} \tag{16}$$

In the case when both T_1 and T_2 weightings are very small,

$$T_R \gg T_1(T) \quad \text{and} \quad T_E \ll T_2(T). \tag{17}$$

Then both Eqs. (9) and (16) reduce to

$$\frac{\partial \ln M(T_E, T)}{\partial T} = -\left(\frac{1}{T}\right)_{T_E \ll T_2(T), T_E \to 0} \tag{18}$$

as in the case of equilibrium nuclear magnetization.

Eqs. (9) and (16) are also applicable to a multi-echo spin-echo sequence and a free induction decay, respectively, In a multi-echo experiment, the echo time, T_E, in Eq. (9) can be replaced by the decay time of the outer envelope of the echo train, $t = 2n\tau$, where n is the number of echoes and 2τ is the echo spacing. In a free induction decay experiment, the echo time in Eq. (16) can simply be replaced by the decay time of the FID.

The temperature dependence of the transverse magnetization for the outer envelope of a Carr–Purcell Meiboom–Gill (CPMG) [6,7] pulse sequence in terms of relaxation rate can thus be written (in the absence of T_1 weighting) as

$$\frac{\partial M(t, T)}{\partial T} = \left(-\frac{1}{T} - t\frac{\partial R_2(T)}{\partial T}\right)M(t, T), \tag{19}$$

where $t = 2n\tau$ is the decay time corresponding to each of the subsequent echoes in a CPMG echo train. We define the following nuclear thermal coefficients as

$$\beta_T = \frac{\partial T_2(T)}{\partial T}, \quad \Omega_T = \frac{\partial R_2(T)}{\partial T}, \qquad \alpha_T = \frac{\partial T_1(T)}{\partial T}, \quad \Lambda_T = \frac{\partial R_1(T)}{\partial T}, \tag{20}$$

where β_T and α_T have units of $\mathrm{s\,K^{-1}}$ and Ω_T and Λ_T have units of $\mathrm{s^{-1}\,K^{-1}}$.

β_T is positive and Ω_T is negative for many substances at ordinary temperatures, and as a result Eq. (19) predicts the following three cases, may arise, depending on the decay time t.

$$\frac{\partial M(t, T)}{\partial T} < 0, \quad t < t_0, \tag{21a}$$

$$\frac{\partial M(t, T)}{\partial T} \approx 0, \quad t \approx t_0, \tag{21b}$$

$$\frac{\partial M(t, T)}{\partial T} > 0, \quad t > t_0, \tag{21c}$$

where t_0 is the critical decay time given by setting Eq. (19) equal to zero.

$$t_0 = -\frac{1}{T\Omega_T}. \tag{22}$$

The temperature dependence of signal appears very weak when the decay time is comparable to t_0 as given in Eq. (21b). For $t < t_0$ the contribution from equilibrium nuclear magnetization is dominant and the temperature dependence of signal is negative whereas for $t > t_0$ the contribution from the transverse relaxation is dominant and the temperature dependence of signal is positive [8,9].

In a spin echo experiment with both T_1 and T_2 weighting, Eq. (7) becomes

$$\frac{\partial \ln M(T_E, T_R, T)}{\partial T} = -\frac{1}{T} + \frac{T_E\beta_T}{T_2^2(T)} - \frac{T_R\alpha_T E_2}{T_1^2(T)}, \tag{23}$$

where $E_2 = E_1/(1 - E_1)$, and in terms of relaxation rates

$$\frac{\partial \ln M(T_E, T_R, T)}{\partial T} = -\frac{1}{T} - T_E\Omega_T + T_R\Lambda_T E_2 \tag{24}$$

as a function of nuclear thermal coefficients and pulse sequence parameters. Using Eq. (24), we now have

$$-\frac{1}{T} - T_E\Omega_T + T_R\Lambda_T E_2 = 0 \quad \Rightarrow \quad (T_E)_0 = T_E = -\frac{1}{T\Omega_T} + T_R E_2\frac{\Lambda_T}{\Omega_T} \tag{25}$$

the critical echo time, $(T_E)_0$, in a $T_1(T)$ and $T_2(T)$ weighted spin-echo experiment as

$$(T_E)_0 = t_0 + t'_0, \tag{26}$$

where $t_0 = -1/T\Omega_T$ as given in Eq. (22) and $t'_0 = T_R E_2 \Lambda_T/\Omega_T$. The first term on the right side of Eq. (26) comes from $T_2(T)$ weighting and the second term comes from $T_1(T)$ weighting in a spin-echo sequence.

A plot of $\partial M(t,T)/\partial T$ vs t in Eq. (19) yields curves with different slopes for different substances as

$$\frac{\partial^2 M(t,T)}{\partial t \partial T} = \left(\frac{R_2(T)}{T} - \frac{\partial R_2(T)}{\partial T} + tR_2(T)\frac{\partial R_2(T)}{\partial T}\right) M(t,T) \tag{27}$$

And a plot of $\partial \ln M(t,T)/\partial T$ versus t gives a line with a slope equal to the negative of the nuclear thermal coefficient, $-\Omega_T$, for the substance as

$$\frac{\partial}{\partial t}\left[\frac{\partial \ln M(t,T)}{\partial T}\right] = -\frac{\partial R_2(T)}{\partial T}. \tag{28}$$

In conventional imaging, gradients are applied for spatial encoding and rapid diffusion of nuclei within these gradients may in principle lead to additional signal losses. These losses could in turn be temperature dependent because the rate of Brownian motion changes with temperature. In practive, however, for human imaging such effects are negligible except when there are large intrinsic variations of magnetic susceptibility within the sample or diffusion sensitizing gradients are deliberately applied. The effects of temperature on the magnitude of NMR signals largely derive from the temperature dependences of the equilibrium nuclear magnetization and relaxation. These effects are verified experimentally for a number of substances and the results are given in the next section.

3. Experiments

The temperature dependence of transverse magnetization as a function of echo time was evaluated using a CPMG pulse sequence for a number of substances in this study. A Bruker Avance 85 MHz ^{1}H NMR system with a 2.0 T superconducting magnet was used. A birdcage coil of 50 mm diameter was used for RF transmission and receiving. The 90° pulse length was 100 μs, the bandwidth was 100 kHz, the number of echoes (n) was 256 in each CPMG sequence, and the echo spacing (2τ) ranged from 0.242 to 5 ms depending on the substance. The time for the acquisition of data for each experiment ranged from 62 to 1280 ms depending on the substance. A total of 30 experiments with an experimental repetition time of 23 s were performed for all the substances. The substances studied were H_2O, H_2O–25% D_2O, H_2O–50% D_2O, H_2O–75% D_2O, $C_2H_4(OH)_2$, $C_3H_5(OH)_3$, H_2O–98.4% H_2SO_4, H_2O–3% Agarose, H_2O–0.2 mM $MnCl_2$, and mineral oil. The deuterated solutions were chosen explicitly to vary the proton density (equilibrium magnetization) without altering the chemical shift. Temperature variations in the samples were controlled by heating and cooling using an air current passing over the sample in the spectrometer. A cylindrical cell with a diameter of 1 cm was used in the experiments. The sample size was 5 mL for all the substances. The temperature variation in the thermal cell was verified using measurements of the proton resonance frequency shift of water [10] and it was varied from 278.2 to 287.1 K over the course of the experiment for each substance. The $T_2(T)$ measurements are based on the integrated behavior of the protons in the substances having multiple resonance lines. The temperature dependence of magnetization was determined using a 300 MHz ^{1}H NMR system. $T_1(T)$ and $T_2(T)$ were measured using inversion recovery spin-echo and multi-echo spin-echo sequences, respectively. The sequence parameters such as inversion time, echo time, and repetition time were adjusted for each of the substances based on their relaxation times.

4. Results

All the substances were subjected to a controlled transient thermal change in which the temperature of the substances was varied slowly over time.

Fig. 1 shows the corresponding variations of $M(0,T)$, $T_2(T)$, $R_2(T)$, and temperature T in water as a function of time t_T, the time of the thermal process.

For $T_R \gg T_1(T)$, the logarithmic time dependence of transverse magnetization in Eq. (6) shows a weak depen-

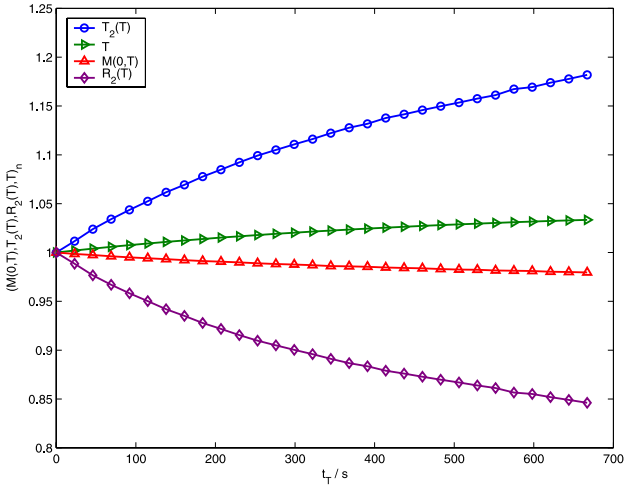

Fig. 1. Experimental variation of normalized $M(0,T)$, $T_2(T)$, $R_2(T)$ and T in a H_2O sample vs. time in a controlled transient thermal experiment in a 2 T magnet.

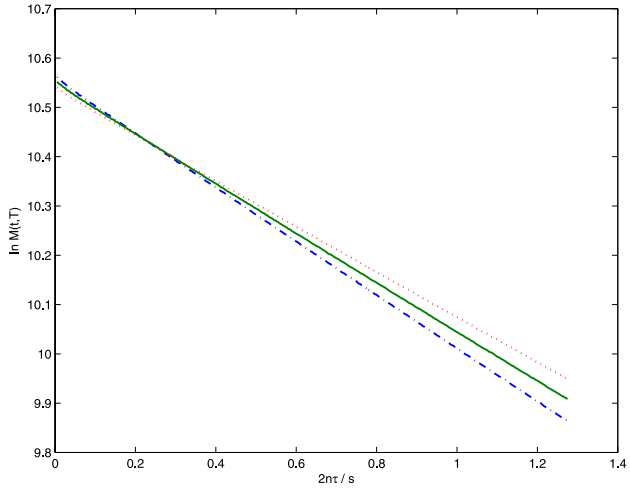

Fig. 2. Experimental logarithmic transverse magnetization (in a.u.) vs decay time in a CPMG sequence at three different temperatures for a H_2O sample in a 2 T magnet.

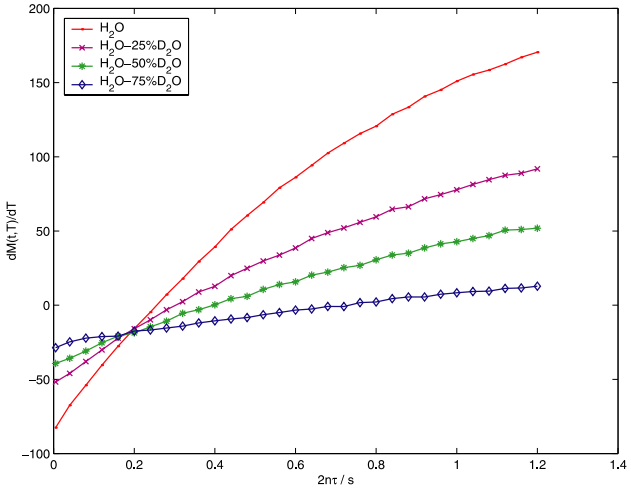

Fig. 3. Experimental temperature dependence of transverse magnetization (in a.u.) vs decay time for H_2O–D_2O mixtures in a 2 T magnet. Substituting D_2O for H_2O reduces the value of $M(0,T)$. $\partial M(t,T)/\partial T$ vary with $t = 2n\tau$ by Eq. (19) and the slopes vary by Eq. (27) for the substances.

dence on the temperature at $t \approx t_0$ as shown by the experimental data for a water sample in Fig. 2.

The slope of each curve in Fig. 2 is equal to $-R_2(T)$ as a function of temperature and the magnitude of the slope decreases with increasing temperature as a result of decreasing $R_2(T)$ for water.

Table 1 shows the experimental data for the temperature dependences of both $T_2(T)$ and $R_2(T)$ in terms of nuclear thermal coefficients, β_T and Ω_T, for a number of substances. Eq. 19 predicts that the temperature dependence of the transverse magnetization in a CPMG sequence will be negative for early echoes but will increase for later echoes, depending on the relative sizes of the various terms.

The experimental temperature dependences of transverse magnetization, $\partial M(t,T)/\partial T$, as a function of $t = 2n\tau$ for various H_2O–D_2O mixtures are given in Fig. 3.

The effect of decay time on the temperature dependence of NMR signal is further demonstrated experimentally by plotting the magnitude of the transverse magnetization for three different echoes corresponding to three cases of the decay times ($t < t_0$, $t \approx t_0$, and $t > t_0$) vs temperature using a H_2O sample as shown in Fig. 4.

The logarithmic temperature dependence of NMR signal varies linearly with decay time for all the substances in Table 1, and the experimental data only for H_2O–D_2O mixtures are shown in Fig. 5.

The $\partial \ln M(t,T)/\partial T$ were linearly regressed against $t = 2n\tau$ using the experimental data in Fig. 5, and $R_2(T)$ was regressed against T using the data in Fig. 6, for each of the H_2O–D_2O mixtures. The experimental regression parameters are given in Table 2.

Table 1
Experimental nuclear thermal coefficients (β_T and Ω_T) and critical decay time (t_0) at a reference temperature (T^0) for several substances in a 2 T magnet

Substance	T^0 (K)	β_T (s K^{-1})	Ω_T (s^{-1} K^{-1})	t_0 (ms)
H_2O	294	0.03479	−0.00864	393.67
H_2O–25% D_2O	294	0.03268	−0.00602	565.01
H_2O–50% D_2O	294	0.04096	−0.00555	612.85
H_2O–75% D_2O	294	0.04828	−0.00400	850.34
$C_2H_4(OH)_2$	294	0.00825	−0.14876	22.86
$C_3H_5(OH)_3$	294	0.00032	−2.48730	1.36
H_2O–98.4% H_2SO_4	294	0.01856	−0.03497	97.26
H_2O–3% agarose	294	0.00017	−0.07121	47.76
H_2O–0.2 mM $MnCl_2$	294	0.00269	−0.07722	44.04
Mineral oil	294	0.00527	−0.25054	13.57

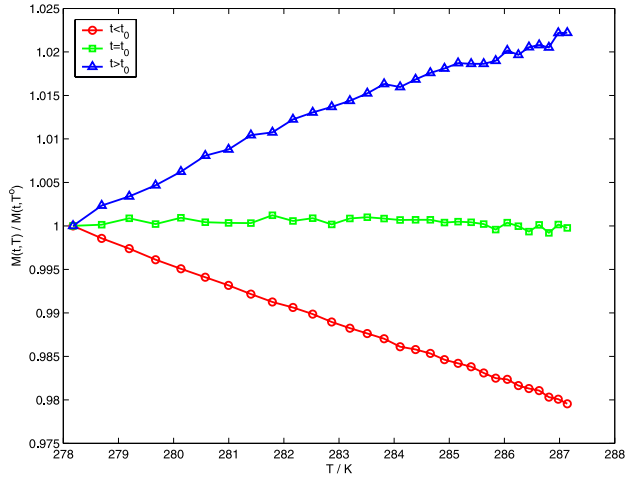

Fig. 4. Experimental normalized magnitude of transverse magnetization vs temperature at three different decay times ($t < t_0$, $t \approx t_0$, and $t > t_0$) corresponding to 1st, 50th, and 100th echo in a CPMG pulse sequence with echo spacing of 5 ms for a H_2O sample in a 2 T magnet.

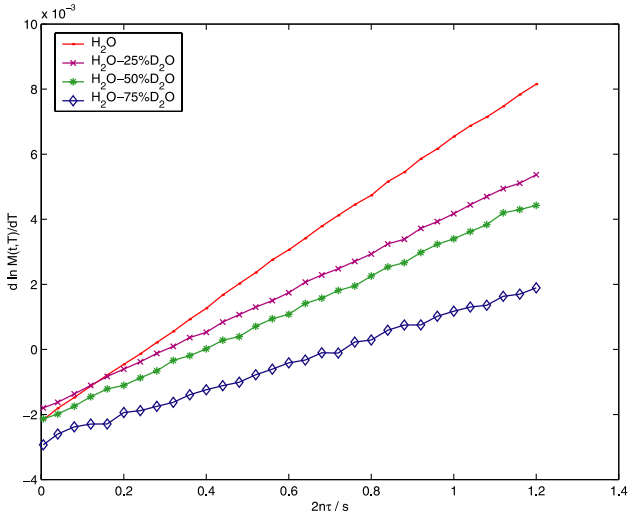

Fig. 5. The experimental logarithmic temperature dependence of transverse magnetization (in a.u.) vs decay time in a CPMG pulse sequence for H_2O–D_2O mixtures in a 2 T magnet. The slopes of lines are equal to $-\Omega_T$ for the substances.

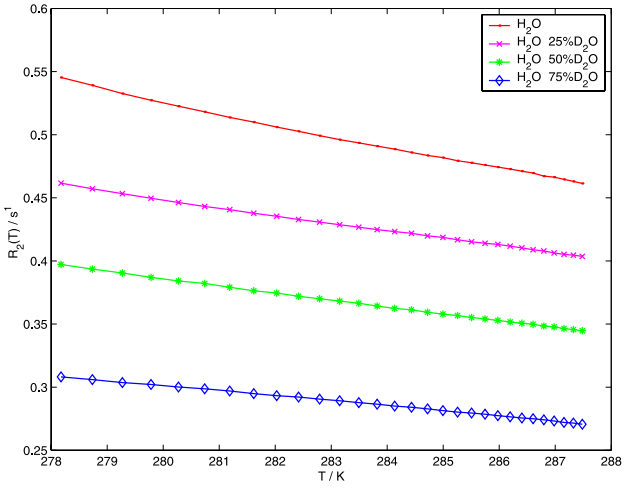

Fig. 6. The experimental transverse relaxation rate vs temperature for H_2O–D_2O mixtures in a 2 T magnet. The slopes of the curves are equal to the nuclear thermal coefficients, Ω_T, for the substances.

Table 2
Experimental linear regression parameters for H_2O–D_2O mixtures in a 2 T magnet

Substance	$R_2(T)$ (s^{-1})	$\partial \ln M(t,T)/\partial T$ (K^{-1})
H_2O	$-0.00864T + 2.94452$	$0.00864t - 0.00215$
H_2O–25% D_2O	$-0.00602T + 2.13522$	$0.00602t - 0.00184$
H_2O–50% D_2O	$-0.00555T + 1.94116$	$0.00555t - 0.00217$
H_2O–75% D_2O	$-0.00400T + 1.42339$	$0.00400t - 0.00284$

The logarithmic temperature dependence of the magnitude of FID signal vs decay time for a H_2O sample in a non-uniform magnetic field in a 7.0 T magnet is shown in Fig. 7 and the plot of $R_2^*(T)$ vs T is shown in Fig. 8.

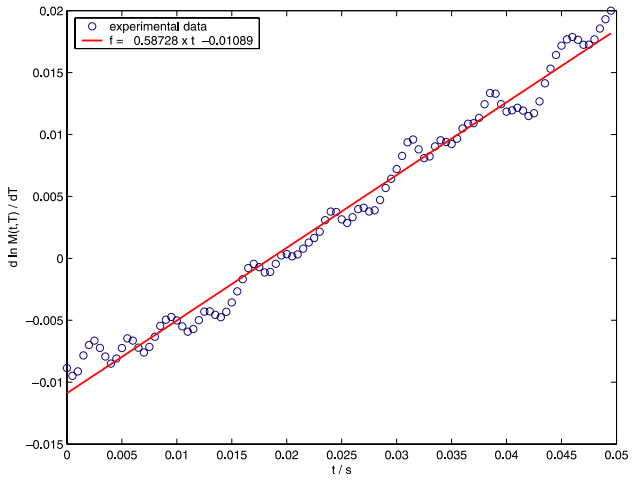

Fig. 7. Experimental logarithmic temperature dependence of transverse magnetization in a FID vs decay time for a H_2O sample in a non-uniform magnetic field in a 7 T magnet. The slope is equal to $-\Omega_T^*$.

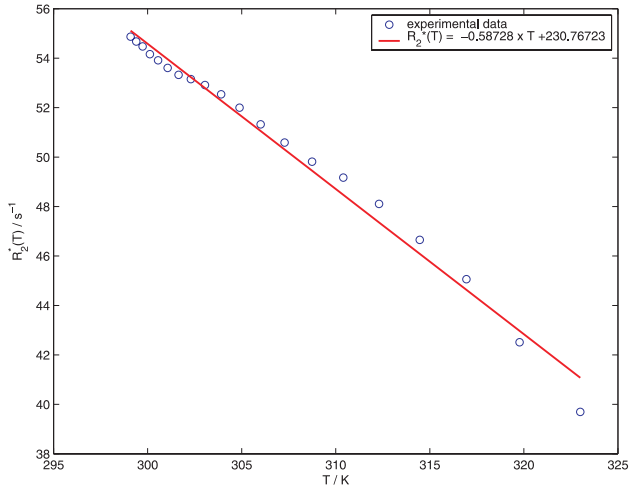

Fig. 8. Experimental transverse relaxation rate in a FID vs temperature for a water sample in a non-uniform magnetic field in a 7 T magnet. The slope is equal to Ω_T^*.

The linear equations, $\partial \ln M(t,T)/\partial T = 0.58728t - 0.01089$ and $R_2^*(T) = -0.58728T + 230.76723$, found through a linear regression of the experimental data, are plotted (solid lines) along with experimental data (circles) in Figs. 7 and 8, respectively.

The temperature dependence of the magnitude of NMR signal in a gradient-echo imaging sequence is experimentally demonstrated with samples of ethylene glycol and glycerol. The GRE imaging parameters are: $T_E = 7$ ms, $T_R = 90$ ms, $\theta = \pi/4$, 128×128, FOV = 8 cm, BW = 12.5 kHz, and $\Delta z = 4$ mm. The GRE magnitude images and spatially averaged magnitudes of NMR signals vs temperature for ethylene glycol and glycerol are shown in Fig. 9.

For reference, the $T_1(T)$ and $T_2(T)$ were measured as 786 and 347 ms for ethylene glycol and 126 and 21 ms

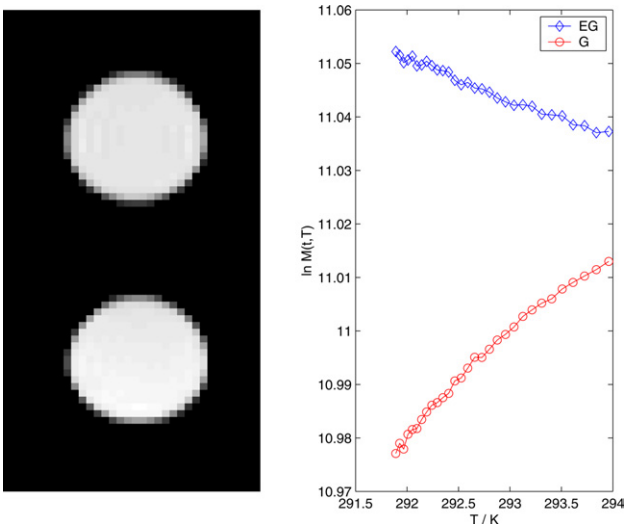

Fig. 9. GRE magnitude images of ethylene glycol (top) and glycerol (bottom). The temperature dependence of the magnitude of NMR signal is negative for ethylene glycol and positive for glycerol in GRE imaging (TE/TR 7/90 ms).

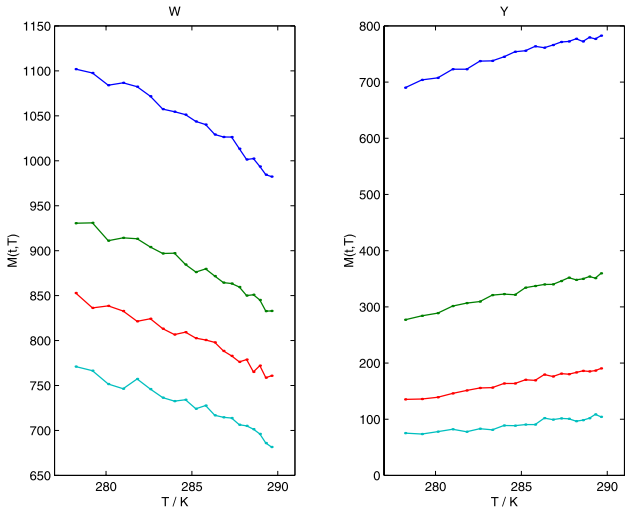

Fig. 11. The variation of NMR signal for egg white (left) and egg yolk (right) with temperature. The curves (from top to bottom) correspond to echo times of 15, 30, 45, and 60 ms, respectively. The temperature dependence of NMR signal is negative for egg white and positive for egg yolk in SE imaging (TE = 15, 30, 45, and 60 ms and TR = 800 ms).

for glycerol at 294 K using inversion recovery spin-echo and multi-echo spin-echo sequences, respectively.

The temperature dependence of the magnitude of NMR signal in a spin-echo imaging is demonstrated with a whole egg. The SE magnitude image of a whole egg is given in Fig. 10.

The SE sequence parameters are: $T_E = 15$, 30, 45, and 60 ms, $n_E = 4$, $T_R = 800$ ms, 128×128, FOV = 12 cm, BW = 12.5 kHz, and $\Delta z = 4$ mm.

The spatially averaged magnitudes of NMR signals from SE images acquired at the echo times of 15, 30, 45, and 60 ms for egg white and egg yolk are plotted vs temperature in Fig. 11.

The average $T_1(T)$ was measured as 1447 and 224 ms using an inversion recovery fast spin-echo sequence and $T_2(T)$ was measured as 138 and 25 ms using a multi-echo spin-echo sequence for egg white and egg yolk at 293 K, respectively.

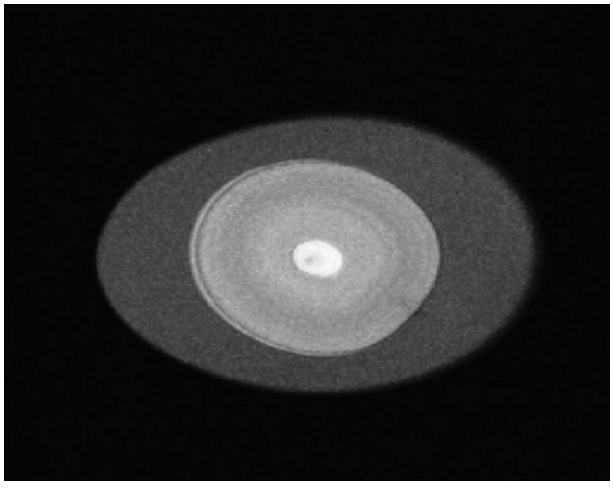

Fig. 10. SE magnitude image of a whole egg. The egg white and egg yolk are subjected to a temperature variation.

5. Discussion

The effect of temperature on the magnitude of the NMR signals measured using common sequences largely derives from the temperature dependences of the equilibrium nuclear magnetization and relaxation rates. The NMR signal is proportional to nuclear magnetization and often depends on relaxation rates, so it is important to take account of the effects of temperature on both of these contributions to account for temperature related changes in the magnitude of the signal. Although the temperature dependence of the equilibrium magnetization is negative, the temperature dependence of transverse relaxation time is positive for a large number of substances at ordinary temperatures and as a result the magnitude of the NMR signal may decrease, increase or stay somewhat constant with increasing temperature depending on the experimental parameters. The experimental parameters are not themselves temperature dependent but they modify the negative and the positive terms in the temperature dependent signal equations. This behavior of the temperature dependences of the magnitudes of NMR signals has been experimentally verified for a number of substances using a multi-echo spin-echo pulse sequence (CPMG), a free induction decay (FID), a spin-echo (SE) imaging, and a gradient-echo (GRE) imaging.

The substances in Table 1 were selected to represent a range of thermal and NMR properties for analysis.

These samples have different spin densities and relaxation times and chemical compositions and represent distinct temperature dependences of both the equilibrium magnetization and relaxation rates. The H_2O–D_2O solutions are used to illustrate the effects of different spin densities and relaxation times.

Since Ω_T is negative for all the substances in Table 1, the second term in parentheses in Eq. (19) is positive and the temperature dependence of transverse magnetization, $\partial M(t,T)/\partial T$, is negative at low $t = 2n\tau$ and positive at high $t = 2n\tau$ and it increases with increasing $t = 2n\tau$. The term $\partial M(t,T)/\partial T$ is negative when $t < t_0$ and positive when $t > t_0$ for each of the substances.

The variations of $\partial M(t,T)/\partial T$ with $t = 2n\tau$ for curves in Fig. 3 are given by Eq. (19) and the slopes of the curves are given by Eq. (27). The slopes decrease with increasing decay time, $t = 2n\tau$, as seen from Eq. (27) and the plots of the experimental data for H_2O–D_2O mixtures in Fig. 3.

As can be seen from the experimental data for water given in Fig. 4, the magnitude of the NMR signal for transverse magnetization can decrease, increase or stay somewhat constant with increasing temperature depending on the echo time or decay time. The magnitudes of signals were taken from the 1st echo, 50th echo, and 100th echo in a CPMG sequence ($2\tau = 5$ ms) corresponding to three cases of the decay times ($t < t_0$, $t \approx t_0$, $t > t_0$), normalized for a reference temperature ($T = 278$ K) and plotted vs temperature. For $t \approx t_0$ the temperature dependence of signal appears very weak as shown for the 50th echo in Fig. 4. This is especially important in thermal imaging where attempts are made to measure the temperature through the transverse relaxation rate $R_2(T)$ by using only a few echoes near t_0. Choosing a few echoes with echo times in the neighborhood of t_0 will exhibit a weak temperature dependence of the signal and therefore β_T or Ω_T will not be measured accurately. Therefore, echo times much smaller ($t \ll t_0$) or much larger ($t \gg t_0$) than the critical decay time are necessary to observe a significant temperature dependence of the signal.

The experimental data for H_2O–D_2O mixtures are given in Table 2, Figs. 5 and 6.

The slopes of the curves in Fig. 5 are equal to $-\Omega_T$ as given by Eq. (28), and the slopes of the curves in Fig. 6 are equal to Ω_T for each of the H_2O–D_2O mixtures.

The slope of the curve in Fig. 7 is then equal to $-\Omega_T^*$ and the slope of the curve in Fig. 8 is equal to Ω_T^*, the temperature dependence of $R_2^*(T)$ for a H_2O sample.

Substances may have different nuclear thermal coefficients and exhibit different temperature dependences of their NMR signals. Under fixed experimental parameters such as echo time and repetition time, the NMR signal can decrease for one substance and increase for another substance during heating depending on the nuclear thermal coefficients of the substances. This may introduce a thermally induced contrast between the substances. For example, using an echo time of 7 ms and a repetition time of 90 ms in a gradient-echo imaging, the magnitude of the signal decreases for ethylene glycol and increases for glycerol with increasing temperature (Fig. 9). The temperature dependence of the signal exhibits $T_1(T)$ and $T_2(T)$ weighting for ethylene glycol (Eq. (14)), but $T_2(T)$ weighting for glycerol (Eq. (16)). The temperature dependence of NMR signal in a spin-echo imaging is also demonstrated with two distinct substances using a whole egg. The magnitudes of the signals at the echo times of 15, 30, 45, and 60 ms and a repetition time of 800 ms decrease in egg white and increase in egg yolk with increasing temperature. At these parameters the temperature dependence of the signal shows $T_1(T)$ and $T_2(T)$ weighting for egg white (Eq. (7)) and $T_2(T)$ weighting for egg yolk (Eq. (9)).

The temperature dependence of NMR signal in imaging and spectroscopy is very important in a number of applications especially in diagnosis and thermal treatment of cancer in oncology. A detailed understanding of the temperature dependence of NMR signal can enhance the accuracy of monitoring thermal effects using NMR imaging. With a complete understanding of the roles of different contributions to the effects of temperature on NMR signal, the pulse sequence parameters such as echo time and repetition time can be optimized for accurate temperature monitoring.

6. Conclusion

The temperature dependence of the magnitude of the NMR signal acquired in common imaging sequences essentially derives from the temperature dependence of the equilibrium nuclear magnetization and relaxation rates. The effect of temperature on the equilibrium nuclear magnetization is significant and should be considered when analyzing NMR images. Using the spin-echo and gradient-echo pulse sequences, the magnitudes of NMR signals can decrease, increase or stay somewhat constant with increasing temperature depending on the combination of parameters such as temperature, echo time, repetition time, relaxation times, and the temperature dependences of relaxation times in substances. The magnitudes of NMR signals vary with temperature in pulse sequences in a systematic manner. Predictions about the temperature dependences of NMR signals can be made on the basis of nuclear thermal coefficients and experimental parameters in various pulse sequences.

Acknowledgments

This work was supported by NIBIB Grant EB00216 awarded to J.C.G. We thank the Yale NMR support group (Terry Nixon, Peter Brown, and Scott McIntyre),

for assistance with the instrumentation and experimentation, and Drs. Mark Does, Dan Gochberg, Jim Joers, Chris Gatenby, and Bruce Damon for helpful comments about data acquisition on the NMR system.

References

[1] N.F. Ramsey, Magnetic shielding of nuclei in molecules, Phys. Rev. 78 (6) (1950) 699–703.
[2] P. Langevin, Magnétisme et théorie des électrons, in: Œuvres Scientifiques de Paul Langevin, CNRS, Paris, 1950, pp. 331–368.
[3] P. Curie, Propriétés magnétiques des corps a diverses températures, Ann. Chim. Phys. 7 (5) (1895) 289–405.
[4] F. Bloch, Nuclear induction, Phys. Rev. 70 (7–8) (1946) 460–485.
[5] E.L. Hahn, Spin echoes, Phys. Rev. 80 (4) (1950) 580–594.
[6] H.Y. Carr, E.M. Purcell, Effects of diffusion on free precession in nuclear magnetic resonance experiments, Phys. Rev. 94 (3) (1954) 630–638.
[7] S. Meiboom, D. Gill, Modified spin-echo method for measuring nuclear relaxation times, Rev. Sci. Instrum. 29 (8) (1958) 688–691.
[8] D.H. Gultekin, A study of thermophysical properties of substances by nuclear magnetic resonance, Ph.D. thesis, Yale University, New Haven, CT, 2002.
[9] D.H. Gultekin, J.C. Gore, Temperature dependence of nuclear magnetization and relaxation, in: Proceedings of the 46th AAPM Meeting, Medical Physics, vol. 31, No. 6, 2004, p. 1772.
[10] J.C. Hindman, Proton resonance shift of water in the gas and liquid states, J. Chem. Phys. 44 (1966) 4582–4592.